

**A new diamond anvil cell for hydrothermal studies to 2.5 GPa and from 190 to 1200 °C**

W. A. Bassett, A. H. Shen, M. Bucknum, and IMing Chou

Citation: *Review of Scientific Instruments* **64**, 2340 (1993); doi: 10.1063/1.1143931


View online: <http://dx.doi.org/10.1063/1.1143931>

View Table of Contents: <http://scitation.aip.org/content/aip/journal/rsi/64/8?ver=pdfcov>

Published by the [AIP Publishing](#)

---

For all your variable temperature, solid state characterization needs....  
... delivering state-of-the-art in technology and proven system solutions  
for over 30 years!



**MMR**  
TECHNOLOGIES

Solutions for Optical Setups!

Seebeck Measurement Systems

Variable Temperature Microprobe Systems

Hall Measurement Systems

Email: [sales@mmr-tech.com](mailto:sales@mmr-tech.com) Web: [www.mmr-tech.com](http://www.mmr-tech.com) Phone: (650) 962-9622 Fax: (888) 522-1011

# A new diamond anvil cell for hydrothermal studies to 2.5 GPa and from $-190$ to $1200$ °C

W. A. Bassett, A. H. Shen, and M. Bucknum  
*Department of Geological Sciences, Snee Hall, Cornell University, Ithaca, New York 14853*

I-Ming Chou  
*959 National Center, U.S. Geological Survey, Reston, Virginia 22092*

(Received 22 February 1993; accepted for publication 12 May 1993)

A new style of diamond anvil cell (DAC) has been designed and built for conducting research in fluids at pressures to 2.5 GPa and temperatures from  $-190$  to  $1200$  °C. The new DAC has been used for optical microscope observations and synchrotron x-ray diffraction studies. Fringes produced by interference of laser light reflected from top and bottom anvil faces and from top and bottom sample faces provide a very sensitive means of monitoring the volume of sample chamber and for observing volume and refractive index changes in samples that have resulted from transitions and reactions. X-ray diffraction patterns of samples under hydrothermal conditions have been made by the energy dispersive method using synchrotron radiation. The new DAC has individual heaters and individual thermocouples for the upper and lower anvils that can be controlled and can maintain temperatures with an accuracy of  $\pm 0.5$  °C. Low temperatures are achieved by introducing liquid nitrogen directly into the DAC. The equation of state of  $H_2O$  and the  $\alpha$ - $\beta$  quartz transition are used to determine pressure with an accuracy of  $\pm 1\%$  in the aqueous samples. The new DAC has been used to redetermine five isochores of  $H_2O$  as well as the dehydration curves of brucite,  $Mg(OH)_2$ , and muscovite,  $KAl_2(Si_3Al)O_{10}(OH)_2$ .

## I. INTRODUCTION

Diamond anvil cells (DAC) have been used in a wide variety of studies both at room temperature and at high temperatures.<sup>1,2</sup> Shortly after the invention of the DAC in 1959 (Refs. 3 and 4) a simple gasket was developed<sup>5</sup> by drilling a hole in a 50–200  $\mu m$  thick metal foil and placing the foil between the diamond anvils so as to create a sample chamber that could be filled with a fluid or a solid sample or a mixture of fluid and solid. DACs have been used to encapsulate fluids to provide hydrostatic pressures to single-crystal fragments<sup>5–7</sup> and powders<sup>8,9</sup> and to study the solidification of fluids at high pressures.<sup>10–12</sup> A small high-temperature diamond anvil cell capable of pressures up to 3 GPa and temperatures up to 450 °C was developed for single-crystal x-ray diffraction studies.<sup>13</sup>

Until recently, very few studies have been made of hydrothermal reactions or of equations of state of fluids in the DAC.<sup>14–16</sup> The DAC described in this article is designed to make such studies reasonably easy and accurate.

## II. THE NEW STYLE OF DIAMOND ANVIL CELL

The new DAC is similar in design to the cell described by Merrill and Bassett<sup>7</sup> but is three to four times as large (Fig. 1). It consists of two platens with diamond anvils mounted at their centers. The two platens are drawn together by tightening nuts on the threaded ends of three posts, thus applying pressure to a sample held between the diamond anvils. Holes through the centers of the platens allow visual and x-ray access to the sample along the compression axis. Molybdenum wires wrapped around the tungsten carbide seats which support the diamond anvils

serve as heaters (Fig. 2). These can heat the anvils and the sample very uniformly and very constantly to temperatures in excess of  $1200$  °C. Electrical leads for the heaters and the thermocouples are fed through the platens. The volume containing the heaters, the anvils, and the sample can be enclosed and completely surrounded with a gas to prevent oxidation. We have found that a constant flow of a mixture of Ar with 1%  $H_2$  is very satisfactory for this purpose.

The new DAC can also be used for low-temperature work. By introducing liquid nitrogen into the brass chamber that forms the base of the DAC we have been able to lower the sample temperature to  $-132$  °C and by introducing liquid nitrogen directly into the chamber surrounding the anvils, we have achieved temperatures as low as  $-190$  °C. The sample temperature can be controlled by reheating the sample using the resistance heaters and temperature controller to any temperature between  $-190$  °C and room temperature.

The new style of DAC has been designed to incorporate several principles important for application to fluid studies and especially for studies of hydrothermal systems. In the following description, we emphasize these principles.

### A. Dimensional stability of the DAC

The new cell is designed so that there are only three simple members (1/2-in.-diam posts) which carry all of the tensile stress (Fig. 1). These are designed to undergo a minimum of dimensional change as the sample is heated. This is accomplished by (1) isolation from the heat sources, (2) by choice of metal, and (3) by air cooling through the hollow centers of the posts. If dimensional

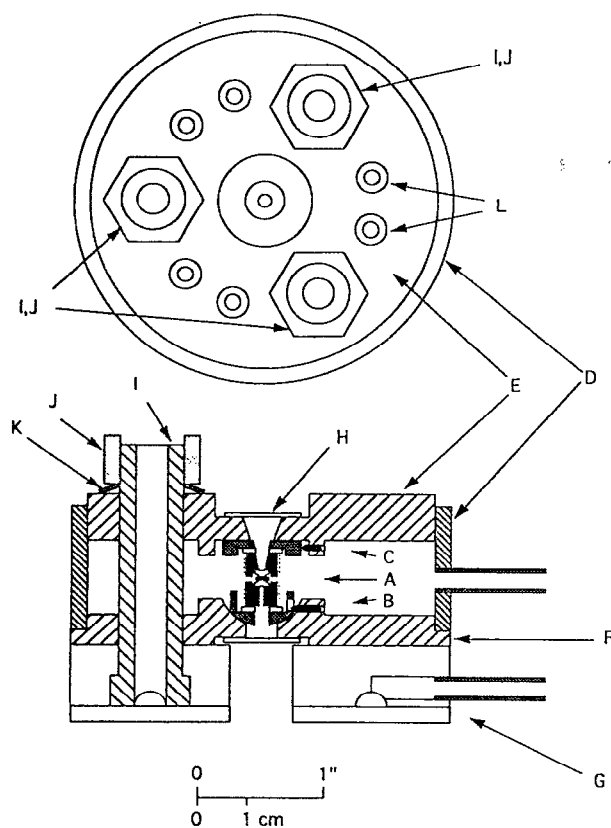


FIG. 1. Plan and elevation of the new diamond anvil cell. The diameter of the cell is 3 in. The height is 2.25 in. The parts are as follows: (A) sample, diamond anvils, heaters, ceramic heat barriers, (B) ball joint for orienting the lower anvil, (C) sliding disk for positioning the upper anvil, (D) cylinder enclosing inert gas chamber, (E) upper platen, (F) lower platen, (G) base with cooling chamber, (H) upper and lower windows (glass or mica), (I) three posts, (J) nuts on threaded parts of posts for applying force, (K) bellville springs, (L) electric feedthroughs. The base is constructed of brass; the platens, posts, and cylinder are constructed of stainless steel.

change proves to be a problem, posts made of other metals can be substituted.

### B. Reliable and secure electric leads

The new DAC is designed to provide very reliable and secure electrical connections for the heater and thermocouple leads. The internal leads for the heaters consist of two heater wires twisted together and running between the feedthroughs and the heaters. External connections are made easily and reliably by means of plugs mounted flush with the surface of the DAC.

### C. Ease of alignment

The diamond anvil seats are mounted on supports designed to make alignment easy and accurate. The lower mount consists of a cradle with a round bottom that fits into a round socket. Three screws with points are driven into holes in the cradle so that the cradle can be rocked by advancing some screws and retracting others. The upper mount consists of a disk positioned by three screws that can be used to slide the upper diamond until it matches the

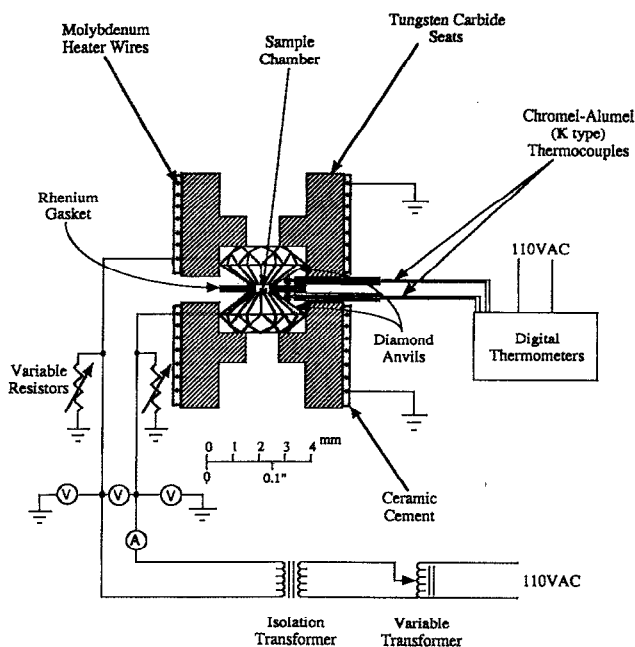


FIG. 2. Schematic diagram showing the method of heating and controlling the temperature of the sample.

lower diamond. The alignment procedures can be done while the DAC is assembled. Fine alignment is accomplished by the positioning of the three nuts on the ends of the posts.

### D. Efficient delivery of heat to the sample

Molybdenum heater wires (0.010 in. in diameter) wound around the tungsten carbide seats deliver heat mainly by direct thermal conduction to the seats and then to the diamond anvils. This approach requires the least input of power and the lowest heater temperature in order to achieve a desired sample temperature.

### E. Precision and accuracy of temperature measurement

The thermocouples (we use chromel-alumel) are cemented so that they are in thermal contact with the upper and lower diamond anvils and are shielded from direct line-of-sight to the heaters as well as the parts of the DAC which are at low temperatures. Thus there is little gain or loss of heat due to radiative transfer to or from other parts of the DAC. Temperature can be measured with a precision of  $\pm 0.1^\circ\text{C}$  over the range of temperature from  $-110$  to  $380^\circ\text{C}$ . The accuracy of our measurements is  $\pm 0.5^\circ\text{C}$  over the same range. At temperatures from  $-190$  to  $-100^\circ\text{C}$  and above  $380^\circ\text{C}$ , the precision is  $\pm 0.5^\circ\text{C}$  and the accuracy is  $\pm 1.5^\circ\text{C}$ .

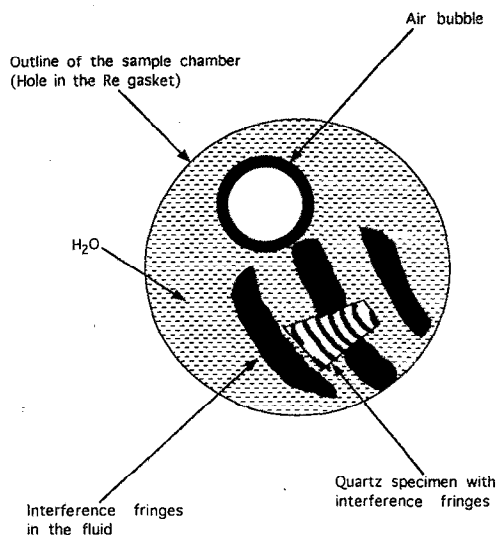


FIG. 3. Typical appearance of a sample of quartz in a mixture of water and air. The portion of the sample illuminated with laser light shows coarse fringes due to interference between light reflected from the two anvil faces. The fine fringes in the quartz sample are caused by interference between light reflected from the top and bottom of the quartz platelet.

#### F. Temperature balance

The power to the upper and lower heaters is controlled individually and the temperatures are measured by individual thermocouples. This allows us to control the temperatures of the two anvils to within less than  $0.1\text{ }^{\circ}\text{C}$  of each other over the temperature range from  $-100$  to  $380\text{ }^{\circ}\text{C}$  and within  $0.5\text{ }^{\circ}\text{C}$  outside of that range.

#### G. Preservation of the heaters and anvils

The heaters, diamond anvils, and all the metal parts that are at high temperature are enclosed in a chamber into which an inert or reducing gas is introduced. This permits the use of molybdenum heating wire which is capable of very high temperatures but is easily oxidized, and it also protects the diamond anvils from oxidation. We use a continuous flow of a gas consisting of a mixture of 1% hydrogen and 99% argon to serve this purpose.

#### H. Visual access

There are two windows that offer visual access to the sample through the diamond anvils and there are two other windows that offer visual access to the sides of the heater assemblage. These windows consist of glass or mica and are transparent to x rays as well as light. We used an optical pyrometer to measure the temperature of the outside surface of the heaters. When the thermocouples indicated  $1250\text{ }^{\circ}\text{C}$ , the optical pyrometer indicated  $1280\text{ }^{\circ}\text{C}$ .

#### I. Sample configuration

Typically the charge loaded into the sample chamber includes a crystal, distilled-de-ionized water, and an air bubble (Fig. 3). The sample chamber is formed by drilling

a  $500\text{-}\mu\text{m}$ -diam hole in a  $125\text{-}\mu\text{m}$ -thick rhenium foil with a Q-switched Nd:YAG laser and then compressing it between two diamond anvils with anvil faces  $1\text{ mm}$  across. The crystal size ranges from  $100\text{ }\mu\text{m} \times 20\text{ }\mu\text{m} \times 20\text{ }\mu\text{m}$  to  $300\text{ }\mu\text{m} \times 300\text{ }\mu\text{m} \times 50\text{ }\mu\text{m}$ .

#### J. Dimensional stability of the sample chamber

The importance of dimensional stability of the sample chamber to the hydrothermal experiments described in this article cannot be overemphasized. The accuracy of our pressure determination depends on the accuracy of temperature measurement and the constant volume conditions of the sample chamber. To verify that the hydrothermal experiments are carried out under constant volume conditions, we have conducted both interferometric and planimetric measurements in an air-filled sample chamber subjected to the same forces as used for samples, and the results show that the variation of the distance between the anvil faces is less than  $0.5\%$  and the lateral dimensions undergo negligible change. Therefore, in the pressure and temperature region of interest, the volume of the sample chamber remains very close to a constant (within  $0.5\%$ ). The crystal in the sample chamber typically occupies less than  $1.5\%$  of the total volume; therefore, the effect of volume change of the crystal at high temperatures and high pressures is negligible. The error due to the inclusion of an air bubble instead of a  $\text{H}_2\text{O}$  vapor bubble is negligible because of the low density of the gas in the air bubble.

### III. CONTROL AND MEASUREMENT OF TEMPERATURE, PRESSURE, AND VOLUME

The upper and lower heaters are in series so that the current is the same in both heaters. The number of windings placed on each of the heaters is the same, and as long as the resistivity of the wire remains constant; the power consumption and therefore the heat output is the same for both heaters. However, minor differences do occur and so we have installed rheostats as shunts across each of the heaters. If the temperature of one of the heaters is higher than the other, we shunt some of the current to an external rheostat thus lowering the heat output of that heater. This method provides an adjustment to an already stable electrical configuration. As a result it permits a very sensitive means of balancing the temperatures of the two heaters so that the temperature difference between the heaters can be controlled within  $\pm 0.1\text{ }^{\circ}\text{C}$  in the range from  $-100$  to  $380\text{ }^{\circ}\text{C}$  and  $\pm 0.5\text{ }^{\circ}\text{C}$  outside of that range.

By providing separate thermocouples for the upper and lower anvils, we are able to carefully monitor the relative temperatures of the two anvils. In order to determine the difference in temperature between the sample location and the thermocouple locations we place a thermocouple between the diamond anvils. When all three thermocouples are monitored, we find discrepancies between the sample location and the thermocouple locations to be less than  $5\text{ }^{\circ}\text{C}$  at temperatures up to  $1200\text{ }^{\circ}\text{C}$ . In practice we calibrate the external thermocouples by observing the melting of calibrants at the sample location. Crystals of  $\text{NaNO}_3$

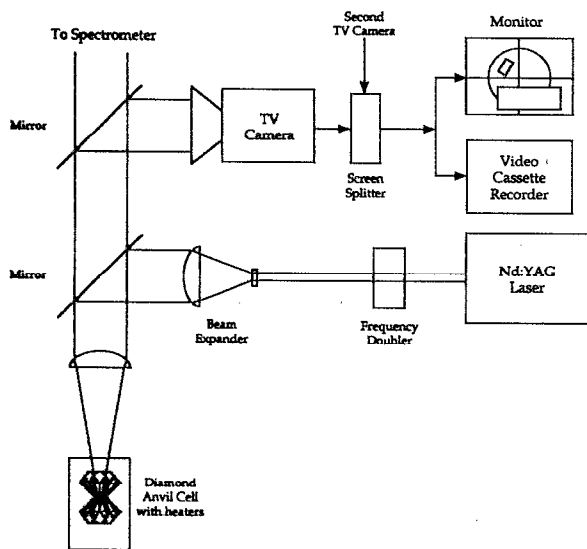


FIG. 4. Schematic diagram showing the optical system for observing and recording interference fringes and changes in the sample. The second TV camera monitors the time and temperatures of the upper and lower anvils. The images from the two TV cameras are displayed simultaneously on the monitor screen. Any visible-light laser would be suitable for this application.

(melting point = 306.8 °C) and NaCl (melting point = 800.5 °C), are placed inside a gasket in the sample location at 1-bar pressure. This method automatically corrects for the discrepancy between the sample and the thermocouples. These thermocouples are not subject to any pressure-induced emf error because they are external and therefore not pressurized. The accuracy of a temperature measurement is believed to be within  $\pm 0.5$  °C between -100 and 380 °C and  $\pm 1.5$  °C outside that range.

A frequency-doubled Nd:YAG laser that produces green light ( $\lambda = 532$  nm) is used as the light source to generate interference fringes for monitoring the optic path (distance times refractive index) between anvil faces. If the fringes do not move with change in temperature and pressure, we assume that the sample has undergone no change in thickness or refractive index. Exactly compensating change in each is extremely improbable. Fringes produced by reflection of light from the top and bottom of a crystal can be observed for abrupt changes in the refractive index and dimensions of the crystal indicating a phase transition. Images from two television cameras, one for direct observation of the sample and the other for digital temperature and time, are superimposed, and recorded on a video cassette recorder (Fig. 4) so that careful analysis of transition temperatures and rate of change can be made at a later time. Other laser sources of visible light prove to be just as satisfactory.

Changes in the interference fringes are usually observed to occur only during the first increase of pressure and temperature. During cooling and decrease of pressure, change may not occur or, if they do occur, may amount to less than a 0.5% change. Subsequent increases and decreases of temperature and pressure typically show no further changes in the fringes. Measurements of the gasket

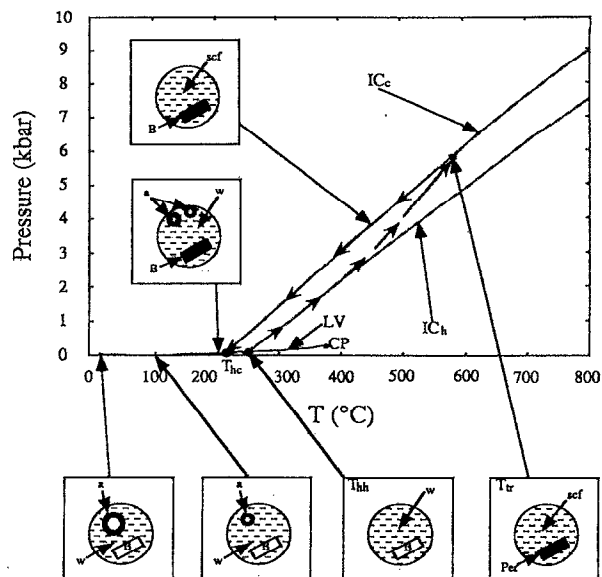


FIG. 5. A typical pressure-temperature path during the observation of a phase transition of a sample immersed in  $H_2O$ . The labels mean the following: (B) brucite [ $Mg(OH)_2$ ] sample, (W) water, (scf) supercritical fluid, a air bubbles, (Per) periclase ( $MgO$ ), (LV) liquid-vapor curve, (CP) critical point, ( $IC_h$ ) isochore at start of heating, ( $IC_c$ ) isochore followed during cooling, ( $T_{hh}$ ) temperature of homogenization measured in the heating cycle, ( $T_{hc}$ ) temperature of homogenization after liquid-vapor separation in a cooling cycle, ( $T_{tr}$ ) temperature of transition. The path drifts from one isochore to another during heating probably due to compression of the gasket. No change in sample volume and therefore density was observed during cooling.

hole before and after indicate that negligible changes take place in the diameter of the hole.

If the sample is more than 32% liquid water, heating the sample chamber causes the liquid to expand and the air bubble to shrink. At the homogenization temperature, the bubble disappears and the sample chamber is filled with the expanded liquid. Further heating of this homogeneous liquid causes the pressure in the sample chamber to increase according to the P-T path of a specific isochore. The density of the isochore is equal to the ratio of liquid to sample chamber volume in the original loading and can be more accurately calculated from the temperature of homogenization along the liquid-vapor curve.

The accuracy of a pressure determination depends on the accuracies of the temperature measurements and the equation of state of  $H_2O$ . The accuracy for our homogenization temperature measurements is believed to be  $\pm 0.5$  °C, which corresponds to a maximum density uncertainty of  $\pm 0.004$  g/cm<sup>3</sup>. The accuracy of the equation of state of  $H_2O$  varies over the range of temperature and pressure studied. Our evaluation of the equations of state of  $H_2O$  that appear in the literature is given in another paper.<sup>16</sup>

#### IV. SOME APPLICATIONS OF THE NEW DAC

##### A. Dehydration of brucite

A single crystal of brucite,  $Mg(OH)_2$ , was placed in distilled, de-ionized water along with a bubble (Fig. 5). By

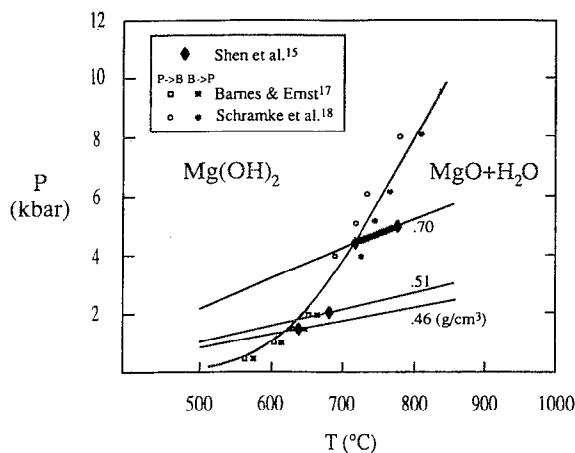


FIG. 6. Pressure-temperature plot of the brucite  $[Mg(OH)_2]$  dehydration curve determined by us compared with determinations reported in the literature. B represents brucite and P represents periclase  $[MgO]$ .

controlling the size of the bubble, we were able to establish the approximate fluid density that would exist at the time of the dehydration. The sample was then heated until the bubble disappeared (homogenization). This is shown as  $T_{hh}$  in Fig. 5. As the sample was further heated, both the temperature and pressure of the homogeneous fluid increased. This was continued until the dehydration reaction  $T_{tr}$  was observed. The dehydration of brucite appeared as a darkening of the crystal in transmitted light. The darkening was caused by scattering of light as dehydration produced interfaces within the crystal. Once this very easily recognized phenomenon was observed, the heating was halted and the sample was cooled along an isochore  $IC_c$  until a vapor bubble reappeared. The sample was then slowly reheated until the vapor bubble disappeared. This was repeated three times, and the temperature at the moment of bubble disappearance  $T_{hc}$  was measured. The isochore density was determined from the homogenization temperature along the liquid-vapor curve and the pressure of dehydration was determined from the temperature of dehydration along the isochore. The resulting dehydration points<sup>15</sup> are shown in Fig. 6 and are compared with the published data of Barnes and Ernst<sup>17</sup> and Schramke *et al.*<sup>18</sup>

### B. Equation of state of water

We have used the hydrothermal DAC to compare the equation of state of  $H_2O$  with the P-T boundary of the  $\alpha$ - $\beta$  transition in quartz. In this case, we used a crystal of quartz polished on top and bottom. The crystal was immersed in water and heated until sudden motion of laser-produced interference fringes was observed indicating the  $\alpha$ - $\beta$  transition. Our results<sup>16</sup> show that the equation of state of  $H_2O$  of Haar *et al.*<sup>19</sup> is in good agreement with the  $\alpha$ - $\beta$  quartz boundary of Mirwald and Massonne<sup>20</sup> for three different isochores (Fig. 7). We have observed that at higher pressures and temperatures the quartz platelets do dissolve in  $H_2O$ . However, this effect of dissolving quartz on the transition pressure is minor because when the quartz dissolves, the volume of the solid is reduced and the

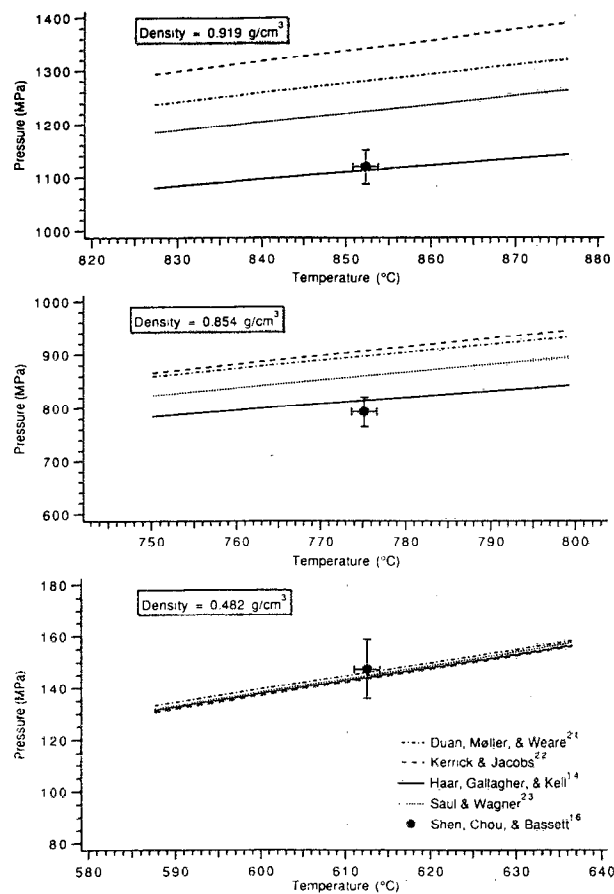


FIG. 7. Measurements of the equation of state of  $H_2O$  at three densities using the  $\alpha$ - $\beta$  quartz transition for calibration. Our data shown by the solid dots with horizontal and vertical uncertainty bars are derived from our  $\alpha$ - $\beta$  quartz transition temperature measurements combined with the transition T-P relationship given by P. W. Mirwald, and H.-J. Massonne (Ref. 21). Our data agree well with those of Haar *et al.* (Ref. 19).

volume of the fluid is increased. The effect that this has on pressure is secondary, due only to the difference between the partial molar volume change during dissolving.

### C. Other applications

We are applying the new diamond anvil cell to an investigation of the morphologies of the various solid phases of  $H_2O$  with the remarkable observation that some of the ice phases crystallize with exceptionally well developed crystal forms. The tetragonal-to-cubic transition in  $BaTiO_3$  is being mapped with the objective of using it as an internal pressure calibrant, much as we have used the  $\alpha$ - $\beta$  transition in quartz.

We have conducted *in situ* diffraction experiments on the Cornell High Energy Synchrotron Source (CHESS). Using a white beam and the energy dispersive method we have followed the dehydration of montmorillonite under pressure at temperatures up to 775 °C. Using a monochromatic beam and the Debye-Scherrer method, we have made some preliminary measurements of the lattice parameters of calcite as a function of pressure and temperature. With these two experiments we have shown that it is pos-

sible to obtain good diffraction data on a polycrystalline sample that is immersed in water at high temperature and pressure.

We have modified the new design of diamond anvil cell for low-temperature work. By introducing liquid nitrogen directly into the brass chamber that forms the base of the diamond cell we have been able to lower the sample temperature to  $-132\text{ }^{\circ}\text{C}$  and by introducing liquid nitrogen into the upper chamber surrounding the anvils we have been able to reduce the temperature to  $-190\text{ }^{\circ}\text{C}$ . These modifications enable us to load carbon dioxide in solid form. It also allows us to measure the temperature of the ice-water transition in  $\text{H}_2\text{O}$  as a function of pressure. This measurement is necessary for studying isochores that have densities in the range  $0.98\text{ g/cm}^3$  to  $1.12\text{ g/cm}^3$ . Densities above  $1.12\text{ g/cm}^3$  can also be measured by means of the ice-liquid transition in  $\text{H}_2\text{O}$  but do not require low temperatures. The capability of controlling and measuring temperatures below  $25\text{ }^{\circ}\text{C}$  is necessary for determinations of the solute concentrations in aqueous solutions through freezing point depression measurements. Therefore, this development is essential to our future studies of the equations of state of aqueous solutions.

The pressures in our experiments did not exceed 2.0 GPa. High pressure-temperature experiments utilizing the constant volume technique can be extended another 1–2 GPa, but such experiments call for higher densities of  $\text{H}_2\text{O}$  and the use of the solid-liquid boundary instead of homogenization for isochore identification. Still higher pressures up to 10 GPa and higher can be achieved with smaller anvil faces but cannot take advantage of the constant volume approach. More traditional pressure measurements based on lattice parameter and fluorescence emission measurements can be used but are less accurate.

## ACKNOWLEDGMENTS

This project was supported by grant EAR9117637 to Bassett and Chou from the National Science Foundation. We wish to acknowledge the help of Tren Haselton, Terry

Wu, and Amy Sun. Critical reviews from Dr. T. Haselton and Dr. G. L. Nord, Jr. at U.S. Geological Survey, Reston, VA are also acknowledged.

- <sup>1</sup>L. C. Ming, M. H. Manghnani, and J. Balogh, in *High-Pressure Research in Mineral Physics*, edited by M. H. Manghnani and Y. Syono (Terra Sci./AGU, Tokyo, Japan/Washington, DC, 1987), p. 69.
- <sup>2</sup>D. Schiferl, J. N. Fritz, A. I. Katz, M. Schaefer, E. F. Skelton, S. B. Qadri, L.-C. Ming, and M. H. Manghnani, in *High-Pressure Research in Mineral Physics*, edited by M. H. Manghnani and Y. Syono (Terra Sci./AGU, Tokyo, Japan/Washington, DC, 1987), p. 75.
- <sup>3</sup>C. E. Wier, E. R. Lippincott, A. Van Valkenburg, and E. N. Bunting, *J. Res. Nat. Bur. Stand.* **63A**, 55 (1959).
- <sup>4</sup>J. C. Jamieson, A. W. Larson, and N. D. Nachtrieb, *Rev. Sci. Instrum.* **30**, 1016 (1959).
- <sup>5</sup>A. Van Valkenburg, *Diamond Res.* **17** (1964).
- <sup>6</sup>R. M. Hazen and C. W. Burnham, *Science* **194**, 105 (1974).
- <sup>7</sup>L. Merrill and W. A. Bassett, *Rev. Sci. Instrum.* **45**, 290 (1974).
- <sup>8</sup>D. R. Wilburn and W. A. Bassett, *Am. Mineral.* **63**, 591 (1978).
- <sup>9</sup>A. P. Jephcoat, H.-K. Mao, and P. M. Bell, *J. Geophys. Res.* **91**, 4677 (1986).
- <sup>10</sup>C. E. Weir, S. Block, and G. J. Piermarini, *J. Res. Nat. Bur. Stand.* **C69**, 275 (1965).
- <sup>11</sup>C. E. Weir, G. J. Piermarini, and S. Block, *Rev. Sci. Instrum.* **40**, 1133 (1969).
- <sup>12</sup>H.-K. Mao and P. M. Bell, *Science* **200**, 1145 (1979).
- <sup>13</sup>R. M. Hazen and L. W. Finger, *Rev. Sci. Instrum.* **52**, 75 (1981).
- <sup>14</sup>A. Van Valkenburg, P. M. Bell, and H.-K. Mao, *Hydrothermal Experimental Techniques*, edited by G. C. Ulmer and H. L. Barnes (Wiley, New York, 1987), p. 458.
- <sup>15</sup>A. H. Shen, W. A. Bassett, and I-Ming Chou, *High-Pressure Research Application to Earth and Planetary Sciences*, edited by Y. Syono and M. H. Manghnani (Terra Sci./AGU, Tokyo/Washington, D.C., 1992), p. 61.
- <sup>16</sup>A. H. Shen, I-Ming Chou, and W. A. Bassett, 29th International Geological Congress, Kyoto, Japan, Aug. 23–Sep. 5, 1992, Abstract Volume, 207 (Abstract, 1992).
- <sup>17</sup>H. L. Barnes and W. G. Ernst, *Am. J. Sci.* **261**, 129 (1963).
- <sup>18</sup>J. A. Schramke, D. M. Kerrick, and J. G. Blencoe, *Amer. Mineral.* **67**, 269 (1982).
- <sup>19</sup>L. Haar, J. S. Gallagher, and G. S. Kell, *NBS/NRC Steam Tables: Thermodynamic and Transport Properties and Computer Programs for Vapor and Liquid States of Water in SI Units* (Hemisphere, Washington D.C., 1984).
- <sup>20</sup>P. W. Mirwald and H.-J. Massonne, *J. Geophys. Res.* **85**, 6983 (1980).
- <sup>21</sup>Z.-H. Duan, N. Møller, and J. H. Weare, *Geochim. Cosmochim. Acta* **56**, 2605 (1992).
- <sup>22</sup>D. M. Kerrick and G. K. Jacobs, *Am. J. Sci.* **281**, 735 (1981).
- <sup>23</sup>A. Saul and W. Wagner, *J. Phys. Chem. Ref. Data* **18**, 1537 (1989).